

Entanglement, state manipulation and quantum-limited metrology with trapped ions

Rainer Blatt^{1,2} and David Wineland³

¹*Institut für Experimentalphysik, Universität Innsbruck, Technikerstr. 25, Innsbruck, Austria*

²*Institut für Quantenoptik und Quanteninformation,*

Österreichische Akademie der Wissenschaften, Otto-Hittmair-Platz 1, Innsbruck, Austria

³*National Institute of Standards and Technology, 325 Broadway, Boulder, Co, USA*

Laser-cooled trapped ions provide a relatively unperturbed system for the creation of entangled states and their manipulation for quantum information processing experiments. Although a general purpose quantum computer remains a distant goal, recent experiments show that a few entangled trapped ions can already be used to advantage in metrology. We describe the basic ingredients that have been used for entanglement and indicate some of the steps needed to scale to larger numbers. If successful, extensions of the demonstrated entangling operations might enable simulations that are intractable on a classical computer.

Introduction

Coherent quantum superposition states of individual particles have been investigated and used for decades in applications such as photon interferometers and Ramsey spectroscopy¹. However, entangled states and particularly entangled states that have been "engineered" or created for specific tasks, have become available routinely only in the last two decades². Early experiments performed

with pairs of entangled photons^{3,4} were important because they provided tests of nonlocality in quantum mechanics⁵. In the 1980s, quantum systems were considered by Feynman and Deutsch as a possible way to perform certain efficient computations or quantum simulations^{6,7}. This idea was largely considered a curiosity until the 1990's when Peter Shor devised an algorithm⁸ that could factor large numbers very efficiently with a quantum computer. This marked the beginning of widespread interest in quantum information processing (QIP) and stimulated a number of proposals for the implementation of a quantum computer⁹⁻¹⁷. Among these, trapped ions⁹ have proven to be one of the most successful avenues for the deterministic creation of entangled states, and for their manipulation, characterization, and use in measurement. There are currently about 25 laboratories worldwide that study various aspects of QIP with trapped ions. Ions provide a relatively “clean” system, because they can be confined for long durations with small environmental perturbations and can be coherently manipulated with laser beams. While this requires a number of technical ingredients, trapped ions thus provide an accessible testing ground for concepts that can also be applied to other systems, such as those employing quantum dots, nuclear spins, superconducting Josephson junctions, photons, neutral trapped atoms, etc.

Quantum information processing with atoms and photons was reviewed in *Nature* by C. Monroe in 2002.¹⁸ Here, we highlight recent advances in the creation and manipulation of ion entangled states, with an emphasis on applications to realizing quantum gates for QIP and their use in improved metrology.

Trapped and laser-cooled ions

To study entanglement, it is desirable to have a system of particles that can be individually manipulated, their internal states entangled, and coherences maintained for long durations, while suppressing the detrimental effects of unwanted couplings to the environment. This can be realized by confining and laser cooling a group of atomic ions in a particular arrangement of electric and/or magnetic fields^{19,20}. With such “traps” atomic ions can be stored nearly indefinitely and localized in space to a few nanometers. Coherence times of ten minutes have been observed for superpositions of two hyperfine states^{21,22}.

In the present context, we typically trap a few ions using a combination of static and sinusoidally oscillating electric potentials applied between the electrodes of a linear quadrupole, called a Paul trap, as shown in Fig. 1. When laser cooled, the ions arrange into a linear “string”, where the spacings are determined by a balance between the horizontal (axial) confining fields and mutual Coulomb repulsion. Scattered fluorescence can be imaged with a camera as shown in the inset of Fig. 1. The use of tightly focused laser beams allows us to address and manipulate individual ions. For simplicity, we focus our attention on two specific internal levels $|g\rangle$ and $|e\rangle$ of each ion. This “qubit” structure is “dressed” by the oscillator states $|n\rangle$ of frequency ω_m of a particular mode (see Fig. 1). We denote the internal states as “spin” states, in analogy with the two states of a spin-1/2 particle, and we’ll first assume that the energy between internal states corresponds to an optical frequency ω_{eg} . This atomic transition can be driven by laser radiation at frequency ω_{eg} , which couples states $|g, n\rangle \leftrightarrow |e, n\rangle$. Spin and motional degrees of freedom can be coupled by tuning the

laser to “sideband” frequencies $\omega_{eg} \pm \omega_m$, which drives transitions $|g, n\rangle \leftrightarrow |e, n + \Delta n\rangle$ ^{23–27}, with $\Delta n = \pm 1$. In this case, state evolution can be described as a rotation $R_{\Delta n}(\theta, \phi)$ of the state vector on the Bloch sphere^{27,28} defined here as

$$\begin{aligned} R_{\Delta n}(\theta, \phi)|g, n\rangle &\longrightarrow \cos\frac{\theta}{2}|g, n\rangle + ie^{i\phi}\sin\frac{\theta}{2}|e, n + \Delta n\rangle \\ R_{\Delta n}(\theta, \phi)|e, n + \Delta n\rangle &\longrightarrow ie^{-i\phi}\sin\frac{\theta}{2}|g, n\rangle + \cos\frac{\theta}{2}|e, n + \Delta n\rangle, \end{aligned} \quad (1)$$

where θ depends on the strength and the duration of the applied laser pulse and ϕ is the laser beam phase at the ion’s position. For $\Delta n = \pm 1$ entanglement is generated between the spin and motional degrees of freedom. Higher-order couplings ($|\Delta n| > 1$) are suppressed for laser-cooled ions whose spatial extent is much smaller than the laser wavelength, the so-called Lamb-Dicke regime. In this regime, “sideband” laser cooling works by tuning the laser to induce absorption on the *lower sideband* ($\Delta n = -1$) followed by spontaneous emission decay, which occurs predominantly at the $\Delta n = 0$ “carrier” transition frequency. With repeated absorption/emission cycles, the ions are optically pumped to the spin/motion ground state $|g, n = 0\rangle$.²⁹ If the spin energy levels correspond to microwave or lower frequencies (as with hyperfine states), the same processes can be realized by replacing single-photon optical transitions with two-photon stimulated-Raman transitions and spontaneous emission with spontaneous Raman scattering.^{24–27}

Resonance fluorescence from an auxiliary state that is strongly coupled (by a monitoring excitation) to one of the qubit levels and decays back only to that same level, allows us to achieve state detection with efficiencies greater than 99 %. This is usually called quantum non-demolition (QND) detection because once the ion is projected into a particular spin state by the excita-

tion/emission cycle, the cycle can be repeated many times and we don't need to detect every emitted photon to achieve good overall detection efficiency. If the qubit is projected to or "shelved" in the state that is not coupled to the fluorescing transition we observe no photons, which can be distinguished from the fluorescing state.³⁰

Spin-Entangled States

In 1995, Ignacio Cirac and Peter Zoller proposed how to use a trapped-ion system to implement a quantum computer⁹. For universal quantum computation and the generation of arbitrary entangled qubit states, two basic gate operations are required: (i) individual qubit rotations as described by Eq. (1), and (ii) a two-qubit entangling operation that enables the realization of the quantum counterpart to a classical logical XOR operation, the so-called controlled-NOT (CNOT) gate operation³¹. The CNOT gate flips the state of a target qubit depending on the state of a control qubit and importantly, when applied to superposition states, it generates entanglement. By the use of individual qubit rotations applied to two trapped ions, the CNOT operation is realized by mapping the state of the control qubit to the common ion motion and using transitions on the target ion which are available if and only if the motion is excited, for details see Fig. 2. As indicated in the lower part of Fig. 2 the CNOT operation in step (2) is achieved with a sequence of carrier ($R_0(\theta, \phi)$) and red sideband pulses ($R_{-1}(\theta, \phi)$). The central part of this sequence is a "phase gate" that applies a phase shift $e^{i\pi} = -1$ to the $|g, 1\rangle$ component of the wave function. This is implemented with a coherent $R_{-1}(2\pi, \phi)$ pulse applied between the $|g, 1\rangle$ state and an auxiliary state $|aux, 0\rangle$. Since the applied radiation cannot excite states $|g, 0\rangle$, $|e, 0\rangle$ or $|e, 1\rangle$, they are un-

affected. This operation is sandwiched between rotations that transfer phase into state changes as in Ramsey spectroscopy. With a single ion Monroe et al. realized the CNOT-operation between motion and ${}^9\text{Be}^+$ spin qubits³²; Schmidt-Kaler et al.^{33,34} and later Riebe et al.³⁵ realized the complete CNOT between two individually addressed ${}^{40}\text{Ca}^+$. Entangling gates have also been realized by irradiating the ions simultaneously (see Fig. 3). Although they can be implemented in a single step, they still involve transitory entanglement with a motional mode, which effectively couples the spin qubits. Ions have also been entangled in a probabilistic way by the coincident detection of scattered photons, for details see Fig. 4.

By sequentially combining single and multi-qubit operations, various entangled states of ions have been created deterministically or “on demand”. In a first experiment, the NIST group created³⁶ the state $\psi_e(\phi) = \frac{3}{5}|ge\rangle - e^{i\phi}\frac{4}{5}|eg\rangle$ where ϕ was a controllable phase factor and $|ge\rangle$ is short for the combined state $|g\rangle_1\otimes|e\rangle_2$ for ions 1 and 2. More generally, using entangling operations and single qubit rotations with adjustable phases, all Bell states $|\Psi^\pm\rangle = \frac{1}{\sqrt{2}}(|ge\rangle \pm |eg\rangle)$, $|\Phi^\pm\rangle = \frac{1}{\sqrt{2}}(|gg\rangle \pm |ee\rangle)$ and arbitrary superpositions can be generated^{37,38}. The quality or fidelity of quantum states is usually characterized by the degree with which they agree with the desired state, which is expressed as

$$F = \langle \psi_{ideal} | \rho_{exp} | \psi_{ideal} \rangle, \quad (2)$$

where ρ_{exp} is the density matrix, which characterizes both pure and non-pure states. In current experiments, fidelities $F > 0.95$ are achieved.

In some cases complete knowledge of the density matrix is not required. For example, the

fidelity of a state relative to $|\Phi^+\rangle$ can be derived from just three matrix elements, $F = \frac{1}{2}(\rho_{gg,gg} + \rho_{ee,ee}) + 2\text{Re}\rho_{ee,gg}$, where $\rho_{ee,gg} \equiv \langle ee|\rho_{exp}|gg\rangle$, etc. The matrix elements $\rho_{gg,gg}$ and $\rho_{ee,ee}$ are obtained from the measured populations of the respective states. We can obtain $\rho_{ee,gg}$ by applying a rotation $R_0(\pi/2, \phi)$ to both ions and measuring the parity $P \equiv (|gg\rangle\langle gg| + |ee\rangle\langle ee| - |ge\rangle\langle ge| - |eg\rangle\langle eg|)$ of the resulting state as a function of ϕ . The only component of the parity that oscillates sinusoidally with frequency 2ϕ is proportional to $\rho_{ee,gg}$, which allows its extraction.³⁹

As shown by Eq. (2), the fidelity can be obtained by a measurement of the full density matrix. For this, the quantum state in question must be prepared many times, and with appropriate single qubit rotations prior to qubit measurements we obtain all expectation values of the density matrix. Such a procedure is known as ‘‘quantum state tomography’’³⁸. When this procedure is applied to Bell states, the density matrix is completely characterized, as shown in Fig. 5. From the density matrices all measures can subsequently be calculated. The expectation value of the operator^{40,41} $A = \sigma_x^{(1)} \otimes \sigma_{x-z}^{(2)} + \sigma_x^{(1)} \otimes \sigma_{x+z}^{(2)} + \sigma_z^{(1)} \otimes \sigma_{x-z}^{(2)} - \sigma_z^{(1)} \otimes \sigma_{x+z}^{(2)}$, where $\sigma_{x\pm z} = (\sigma_x \pm \sigma_y)/\sqrt{2}$. For local realistic theories, measurements of $|\langle A \rangle|$ are predicted to be less than 2, and values of $2 < |\langle A \rangle| < 2\sqrt{2}$ are expected for states that can be described only by quantum theory. With trapped ions, the measured Bell signal was found to be $|\langle A \rangle| = 2.25(3)$ at NIST³⁷ in 2001, $|\langle A \rangle| = 2.52(6)$ at Innsbruck³⁸ and $|\langle A \rangle| = 2.20(3)$ at Michigan⁴² in 2004, clearly corroborating quantum theory. Moreover, each time an experiment was run, a result was recorded. This closed the so-called detection loophole, which provided a way to violate Bell’s inequalities within local realistic theories.

The operations outlined above can be generalized to entangle more than two particles. Among such states, the so-called cat states, named after Schrödinger’s cat⁴³, are of particular interest. Cat states are usually defined as superpositions of two particular maximally different states, such as

$$\psi_{cat} = \alpha|ggg \dots g\rangle + \beta|eee \dots e\rangle \quad (3)$$

and they play a distinguished role in quantum information science. For three qubits, they are also called GHZ states after Greenberger, Horne, and Zeilinger, who showed that they could provide a particularly clear contradiction with local realistic theories⁴⁴. They are a fundamental resource in fault-tolerant quantum computing, for error correction^{45,46} and for quantum communication, where they can enable protocols such as open-destination teleportation⁴⁷ and secret sharing⁴⁸. Because of their sensitivity to the interferometric phase ϕ , they can also enable improved signal-to-noise ratios in interferometry⁴⁹.

With trapped ions, cat states with $|\alpha| = |\beta|$ have been generated by use of two different approaches. At NIST, global entangling operations were used to demonstrate four-ion entanglement in Ref. ³⁹ and a GHZ state with $F = 0.89$.⁵⁰ More recently, the NIST group produced cat states of up to 6 ions via a global entangling operation.⁵¹ Using individually addressed ions and a CNOT-gate operation, the Innsbruck group⁵² produced GHZ states in an algorithmic way, and analyzed the states again via tomographic measurements. In a similar way, yet with another pulse sequence, the Innsbruck group also produced the so-called W states

$$|\psi_W\rangle = \frac{1}{\sqrt{N}}(|g \dots gge\rangle + |g \dots geg\rangle + \dots + |eg \dots g\rangle) \quad (4)$$

that belong to a different class of entangled states. Such classes are distinguished since states of dif-

ferent classes cannot be transformed into each other by local operations and classical communication⁵³. Nevertheless, both cat and W states can violate Bell-type inequalities⁵⁴. As opposed to cat states, W-states are remarkably robust against various decoherence processes; even loss of qubits does not destroy entanglement completely. The Innsbruck group engineered an 8-qubit W-state⁵⁵ using individual ion addressing. Both, the NIST and Innsbruck groups proved multi-partite entanglement using an “entanglement witness”, an operator constructed so that its expectation value must exceed (or be less than) a certain value to verify N -particle entanglement.^{51,55}

Demonstrating QIP algorithms

Algorithms are lists of instructions for completing a task. As in classical computation, quantum algorithms can sometimes be viewed as subroutines in a larger computation. A QIP algorithm will generally involve single- and multi-qubit gates, measurements, and measurement-dependent operations. The result of such a sequence of operations could be either a deterministically prepared quantum state such as a Bell, GHZ, or W state, a conditioned state such as an error-corrected state, or the outcome of a computation that is subsequently inferred from a measurement of the quantum register and is then available as classical information.

Quantum information processing allows one to perform tests using superpositions while classically this ability is absent. A simple example showing the gain in efficiency with a quantum algorithm was proposed in the Deutsch-Jozsa algorithm.⁵⁶ It was first demonstrated on two qubits in NMR,⁵⁷ and more recently with a trapped ion⁵⁸ whose motional and spin qubit served as

the two qubits.

As a second example algorithm, we consider teleportation of one qubit's state to another, an important protocol for the transfer of quantum information (see Ref.⁵⁹ and Box 2 in Ref.¹⁸). Here, Alice wants to send a (in general unknown) qubit state to Bob. To do this, first a Bell pair is generated, and one qubit each from the pair is given to sender Alice and receiver Bob. When the unknown state is ready to be teleported, it is entangled with Alice's qubit of the Bell pair. A subsequent measurement of both qubits by Alice yields two bits of classical information that she sends to Bob. With this information, Bob knows which of four possible rotations to apply to his qubit to obtain Alice's original unknown state.

Deterministic quantum teleportation has been demonstrated by the NIST⁶⁰ and Innsbruck⁶¹ teams. The Innsbruck team used individual laser-beam addressing of three qubits; thus the state was teleported from one other end of the ion string, a distance of about 10 μm . The NIST team used a multi-zone linear trap array. By applying control potentials to electrode segments, the ions could be separated and moved in and out of one zone in which the laser beams were present. Here, the state was teleported across a few hundred micrometers.

Teleportation is an important building block for quantum information processing, and can reduce the resource requirements.⁶² Furthermore, it is the basic procedure for quantum communication protocols, such as for implementing quantum repeaters. Other algorithms, such as entanglement purification⁶³ and error correction⁶⁴, the quantum Fourier transform⁶⁵ and deterministic entanglement swapping,⁶⁶ have also been demonstrated with ion qubits.

While these experiments demonstrate the basic features of quantum algorithms, concatenation of processes and repeated computations will require improved operation fidelities. In particular, full and repetitive implementation of quantum error correction, which could keep a qubit superposition “alive” while subjected to decoherence, remains one of the biggest challenges in quantum information processing.

Applications

Shor’s period-finding algorithm for factoring large numbers⁸ generated the wave of interest for potential applications of QIP in the mid 1990’s. Another noteworthy potential application is the implementation of unstructured searches⁶⁷. However, to be of practical use, these applications require substantial resources in terms of the number of qubits and number of operations, well beyond the capabilities of current or near-term implementations. In spite of this, some elements of QIP and entanglement with small numbers of qubits have already found applications in metrology; physicists also anticipate that useful quantum simulations can be performed on a relatively small number of qubits, perhaps up to 100, in the coming decade.

One application of entanglement in metrology is for interferometry. Here, we discuss applications of entanglement to Ramsey atomic spectroscopy⁶⁸, but this has a direct analog in electron, atom, and photon (Mach-Zehnder) interferometers. Ramsey spectroscopy on the $|g\rangle \rightarrow |e\rangle$ transition proceeds as follows. The atom is first prepared in state $\psi_{initial} = |g\rangle$. Radiation at frequency ω near ω_{eg} is applied in a fast pulse to produce the state $R_0(\pi/2, -\pi/2)|g\rangle = \frac{1}{\sqrt{2}}(|g\rangle + |e\rangle)$. The

atom is now allowed to evolve for a duration T so that the atom's upper state accumulates a phase $\phi_R = (\omega - \omega_{ge})T$ relative to the lower state (where we view the problem in a frame that rotates at frequency ω). Finally, we again apply a rotation $R_0(\pi/2, -\pi/2)$ that leaves the atom in the state (up to a global phase factor)

$$|\psi_{final}\rangle = \sin(\phi_R/2)|g\rangle + i \cos(\phi_R/2)|e\rangle. \quad (5)$$

Therefore, the probability of finding the atom in the state $|e\rangle$ is $P_e = \frac{1}{2}(1 + \cos[(\omega - \omega_{ge})T])$. For an ensemble of N atoms, the detected signal will be NP_e . In precision spectroscopy, we are interested in detecting changes in $\omega - \omega_{ge}$ or ϕ_R , as observed through changes in P_e . Therefore, we can define the N -ion signal as $S = d(NP_e)/d\phi_R = -N/2 \sin(\phi_R)$. The fundamental noise in the signal is given by ‘‘projection noise’’, the fluctuations in the number of atoms, from experiment to experiment, measured to be in the state $|e\rangle$ ⁶⁹. The variance of this noise is given by $\sigma_N = NP_e(1 - P_e)$, so the magnitude of the signal-to-noise ratio is equal to $S/\sqrt{\sigma_N} = \sqrt{N}$, essentially the shot noise corresponding to the number of atoms.

Now suppose we can replace the first $R_0(\pi/2, -\pi/2)$ pulse with an entangling $\pi/2$ pulse^{50,51}, which creates the cat state

$$\begin{aligned} |g\rangle_1 |g\rangle_2 \cdots |g\rangle_N &\rightarrow \frac{1}{\sqrt{2}} [|g\rangle_1 |g\rangle_2 \cdots |g\rangle_N + |e\rangle_1 |e\rangle_2 \cdots |e\rangle_N] \\ &\equiv \frac{1}{\sqrt{2}} [|e_N\rangle + |g_N\rangle]. \end{aligned} \quad (6)$$

After a delay T , the $|e_N\rangle$ state accumulates a phase $N\phi_R$ relative to the $|g_N\rangle$ state. A final entangling $\pi/2$ pulse leaves the atoms in a superposition state $\sin(N\phi_R/2)|g_N\rangle + i \cos(N\phi_R/2)|e_N\rangle$; therefore the probability of detecting the atoms in the $|e_N\rangle$ state is $P_{N_e} = \frac{1}{2}(1 + \cos[N(\omega - \omega_{ge})T])$.

It is as if we have performed spectroscopy on a single “super-atom” whose resonant frequency is N times higher than that of a single atom and has a phase sensitivity (to the N th harmonic) of the applied radiation that is N times higher. This gain in interferometric sensitivity must however be offset by the fact that we are measuring only an effective two-state system, composed of the states $|e_N\rangle$ and $|g_N\rangle$. Nevertheless, when compared to the case of N unentangled atoms, after a statistically significant number of repeated measurements, we gain a factor of \sqrt{N} in sensitivity by using entangling $\pi/2$ pulses^{49–51}. Of course, because of technical noise in the experiments, this full theoretical improvement is not realized,; however, a gain over the case of unentangled atoms has been realized for up to six entangled ions^{51,70,71}.

The above arguments assumed that noise was due only to state projection. In experiments, if correlated qubit phase decoherence is present, the gain may be lost due to the faster decoherence of the cat states⁷², or lost due to noise in the oscillator that produces the radiation^{27,73}. If these sources of noise can be suppressed, entangled states should be able to improve the signal-to-noise ratio in future spectroscopy experiments.

Another application of QIP techniques is enhanced detection fidelity.⁷⁴ This can be useful if the qubit does not have a cycling transition or if the QND aspect of shelving detection is not well satisfied. In one simple implementation, assume we have two qubits, labelled q and d , stored in the same trap. The goal is to detect the state of information-qubit q , using detection-qubit d . Prior to measurement, q will generally be in a superposition state $\alpha|g\rangle_q + \beta|e\rangle_q$. Using the swap operations of the Cirac–Zoller gate, we first transfer this superposition onto the qubit composed of the $|0\rangle$ and

$|1\rangle$ states of a selected motional mode, then map this superposition onto qubit d . We then measure d , thereby effectively measuring qubit q . We can carry out this protocol without disturbing the initial probabilities $|\alpha|^2$ and $|\beta|^2$ for q , even if the mapping steps above are imperfect. Therefore it is a QND measurement and can be repeated to increase detection efficiency. This scheme was demonstrated in an experiment⁷⁵ where qubit q was based on an optical transition in $^{27}\text{Al}^+$ and qubit d was based on a hyperfine transition in $^9\text{Be}^+$. In that experiment, a single round of detection had a fidelity of only 0.85; however by repeating the measurement, and using real-time Bayesian analysis, the detection fidelity was improved to 0.9994. Note that this same strategy can also be used to prepare an eigenstate of q with high fidelity. In addition to this demonstration, the protocol is now used routinely in a high-accuracy optical clock based on single $^{27}\text{Al}^+$ ions⁷⁶. The technique has also been extended so that a single detection qubit measures states of multiple ions⁷⁵, similar to the measurement of photon Fock states with multiple probe atoms⁷⁷.

Finally, entanglement can be used in metrology to create states that allow measurement of certain parameters while suppressing sensitivity to others. In Ref.⁷⁸ this strategy was used to make a precise measurement of the quadrupole moment of the $^{40}\text{Ca}^+$ ion by performing spectroscopy on an entangled state of two ions that depended on the quadrupole moment but was insensitive to magnetic field fluctuations.

Future

More and Better To create many-ion entangled states, it appears that two main issues must be dealt with: improving gate fidelity, and overcoming the additional problems associated with large numbers of ions. The gate fidelity required to reach fault-tolerant operation, which will allow large-scale computation and entanglement, depends on many factors. A reasonable guideline is to assume that the error probability during a single gate should be on the order of 10^{-4} or less. An important benchmark is two-qubit gate fidelity. The current record is an error of somewhat less than 10^{-2} , which can be inferred from the fidelity of Bell state generation⁷⁹. Generally, it appears that gate fidelities are compromised by limited classical control, such as laser beam intensity fluctuations at the positions of the ions, and quantum limits such as decoherence caused by spontaneous emission.⁸⁰ These are daunting technical problems, but with sufficient care and engineering expertise, it appears that they can eventually be suppressed.

The multi-qubit operations discussed above rely on being able to spectrally isolate a single mode of the ions' motion. Since there are $3N$ modes of motion for N trapped ions, as N becomes large, the mode spectrum becomes so dense that the gate speeds must be significantly reduced to avoid off-resonance coupling to other modes. Proposals exist for circumventing this problem^{81,82} but for the near term, and using gates that have been demonstrated, one way to solve it involves distributing the ions in an array of multiple trap zones^{27,83-85} as indicated schematically in Fig. ???. In this architecture, multi-qubit gates could be performed on a relatively small number of ions in multiple processing zones. Entanglement could be distributed between zones by moving ions^{27,84,85},

or by optical means^{83,86–89}. For quantum communication over large distances, optical distribution seems to be the only practical choice; for local entanglement experiments, moving ions is also an option.

Example traps that could be used for scaling are shown in Fig. ???. Ions can be moved between zones by applying appropriate control potentials to the different electrode segments^{60,90–92}. In Ref.⁹⁰, individual ions were moved ~ 1 mm in $\sim 50 \mu\text{s}$ without loss of coherence; heating of the ion’s motion (in its local well) was less than one quantum. Multiple ions in a single zone can be separated^{60,90} by inserting an electric potential wedge between the ions. In the NIST teleportation experiment⁶⁰, two ions could be separated from a third in a duration of $\sim 200 \mu\text{s}$ with negligible heating of their logic “stretch” mode and heating of their center-of-mass mode of the ions by about 1 quantum. This meant that an additional entangling gate operation on the separated ions could be implemented with reasonable fidelity. For algorithms of long duration, the ions will eventually heat from transport and noisy background electric fields. To counteract this, we can employ additional cooled ions whose function is to sympathetically cool the qubits (cf. Fig.??). These “refrigerator” ions could be identical to the qubit ions⁹³, a different isotope⁹⁴, or a different species⁹⁵. They could also double for use in detection and state preparation, as described above. For all multi-qubit gates implemented so far, speeds are proportional to ion mode frequencies, which scale as $1/d_{qe}^2$, where d_{qe} is the distance of the ion to the nearest electrode. This puts a premium on small trap size. Many groups have pushed in this direction, but all observe significant heating of the ions, which compromises gate fidelity. The heating is anomalously large compared to the expected thermal noise heating from resistance in or coupled to the trap electrodes.^{27,96–102} It scales approx-

imately as $1/d_{qe}^4$ ^{99,100}, consistent with independently fluctuating potentials on electrode patches whose extent is small compared to d_{qe} ⁹⁶. The source of the heating is still to be understood, but recent experiments^{97,101} indicate that it is thermally activated and can be significantly suppressed by operating at low temperature.

Large trap arrays will require a robust means of fabrication and independent control of a very large number of electrodes. Microelectromechanical systems (MEMS) fabrication techniques can be employed for monolithic construction^{102,103}. Trap structures can be further simplified by placing all electrodes in a plane^{103,104}. To mitigate the problem of controlling many electrodes, it may be possible to incorporate "on-board" electronics in close proximity to individual trap zones¹⁰⁵. Laser beams must also be multiplexed since it will be essential to perform parallel operations in complex algorithms. Although re-cycling of beams can be employed^{105,106}, in general overall laser power requirements will increase. If gates are implemented by use of stimulated-Raman transitions, high laser beam intensity is also needed to suppress spontaneous emission decoherence to fault-tolerant levels⁸⁰. Detection must also be multiplexed. This might be solved by coupling to fibers, on-board detectors, or other forms of miniature integrated optics.

Future Applications In the early 1980's Richard Feynman suggested that one quantum system could perhaps be used to simulate another⁶. This could be accomplished efficiently with a quantum computer because of its universality, but before this goal is reached, it may be possible to take advantage of the fact that current logic gates are implemented by Hamiltonians that can be used to simulate interactions in other systems. A very simple example is mentioned above in the discussion

of spectroscopy with cat states; these experiments simulate the action of electron, photon or atom Mach-Zehnder interferometers that incorporate nonlinear, entangling beam splitters⁷¹. A more interesting prospect is that the gate Hamiltonians might be applied in a strategic way to simulate specific many-body Hamiltonians. To see the basic idea, we note that the two-ion phase gate discussed in Fig. 5 can be written in the form $R_{Z1}R_{Z2}e^{-i\xi\sigma_{z1}\sigma_{z2}}$, where R_{Zj} is a rotation about the z axis. Therefore, up to an overall rotation on the qubits, the gate implements the Hamiltonian $H = \hbar\kappa\sigma_{z1}\sigma_{z2}$, a spin-spin interaction between the two addressed spins. By extending these couplings to many ion qubits in an ensemble, Ising-type spin Hamiltonians could, for example, be implemented. The interactions could be applied in a stepwise fashion between ion pairs but might also be implemented simultaneously, thereby increasing efficiency.^{107–109} Although still very challenging compared to current experimental capabilities, even with a relatively small number of ions, interesting phenomena such as quantum phase transitions may be observable, stimulating several experimental groups to pursue this avenue.

Summary and Conclusions

We have outlined some basic techniques that enable deterministic entanglement of a few trapped ions. Many groups are currently trying to extend these capabilities to a large number of ions. Although a large-scale entangling machine or a universal quantum computer are still a distant goal, some of the simple elements of QIP can be used to enhance metrology, as in spectroscopy. We have also briefly indicated how a relatively small number of ion qubits might provide useful quantum simulations.

As we progress towards to a large-scale device, it might be possible to shed some light on more fundamental issues of decoherence and why states having the attributes of Schrödinger’s cat aren’t observed. If we can continue scaling to large size, this issue becomes more pressing. For example, suppose that in the future N -qubit cat states in the form of Eq. 6 can be made. We can rewrite this state as $\psi = \frac{1}{\sqrt{2}}[|g\rangle_j \otimes_{i \neq j}^N |g\rangle_i + |e\rangle_j \otimes_{i \neq j}^N |e\rangle_i]$, thereby (arbitrarily) singling out the j th qubit. For large N , this wavefunction indeed has the attributes of a Schrödinger’s cat in the sense that the states of a single two-level quantum system (the j th qubit) are correlated with states that have macroscopically distinct states of polarization. If we are successful, then we’ve in fact shown the existence of what are essentially Schrödinger’s cats. Of course such states become more sensitive to the effects of phase decoherence⁷², but this appears to be a technical, not fundamental, problem. Therefore, if it becomes impossible to make such states or build a large-scale quantum computer for non-technical reasons, this failure may indicate some new physics!

Bibliography

1. Ramsey, N. F. *Molecular Beams* (Oxford University Press, 1956).
2. Vedral, V. Quantifying entanglement. *Nature* **this volume** (2008).
3. Freedman, S. F. & Clauser, J. F. Experimental test of local hidden-variable theories. *Phys. Rev. Lett.* **28**, 938–941 (1972).
4. Aspect, A., Grangier, P. & Roger, G. Experimental tests of realistic local theories via Bell's theorem. *Phys. Rev. Lett.* **47**, 460–463 (1981).
5. Bell, J. S. *Speakable and unspeakable in quantum mechanics* (Cambridge University Press, 1987).
6. Feynman, R. Simulating physics with computers. *Int. J. Theoret. Phys.* **21**, 467 (1982).
7. Deutsch, D. *Proc. R. Soc. Lond. A* **A400**, 97 (1985).
8. Shor, P. W. Algorithms for quantum computation: discrete logarithms and factoring. In *Proceedings of the 35th Annual Symposium on Foundations of Computer Science, Santa Fe, NM, Nov. 20-22, IEEE Computer Society Press, pp. 124–134* (1994).
9. Cirac, J. I. & Zoller, P. Quantum computations with cold trapped ions. *Phys. Rev. Lett.* **74**, 4091–4094 (1995).
10. Pellizari, T., Gardiner, S. A., Cirac, J. I. & Zoller, P. Decoherence, continuous observation, and quantum computing: A cavity QED model. *Phys. Rev. Lett.* **75**, 3788–3791 (1995).

11. Gershenfeld, N. & I.L.Chuang. Bulk spin-resonance quantum computation. *Science* **275**, 350–356 (1997).
12. Loss, D. & DiVincenzo, D. P. Quantum computation with quantum dots. *Phys. Rev. A* **57**, 120 (1998).
13. Kane, B. E. A silicon-based nuclear spin quantum computer. *Nature* **393**, 133–137 (1998).
14. Briegel, H. J., T.Calarco, Jaksch, D., J.I.Cirac & Zoller, P. Quantum computing with neutral atoms. *J. of Mod. Opt.* **47**, 415–451 (2000).
15. Deutsch, I. H., G.K.Brennen & P.S.Jessen. Quantum computing with neutral atoms in an optical lattice. *Fortschritte der Physik* **48**, 925–943 (2000).
16. Knill, E., R.Laflamme & G.J.Milburn. A scheme for efficient quantum computation with linear optics. *Nature* **409**, 46–52 (2001).
17. Makhlin, Y., Schön, G. & Shnirman, A. Quantum-state engineering with Josephson junction devices. *Rev. Mod. Phys.* **73**, 357–400 (2001).
18. Monroe, C. Quantum information processing with atoms and photons. *Nature* **416**, 238–246 (2002).
19. Dehmelt, H. Experiments with an isolated subatomic particle at rest. *Rev. Mod. Phys.* **62**, 525–530 (1990).
20. Paul, W. Electromagnetic traps for charged and neutral particles. *Rev. Mod. Phys.* **62**, 531–540 (1990).

21. Bollinger, J. J., Heinzen, D. J., Itano, W. M., Gilbert, S. L. & Wineland, D. J. A 303-MHz frequency standard based on trapped $^9\text{Be}^+$ ions. *IEEE Trans. Instr. Meas.* **40**, 126–128 (1991).
22. Fisk, P. T. H. *et al.* Very high q microwave spectroscopy on trapped $^{171}\text{Yb}^+$ ions: application as a frequency standard. *IEEE Trans. Instrum. Meas.* **44**, 113–116 (1995).
23. Bergquist, J., Jefferts, S. R. & Wineland, D. J. Time measurement at the millennium. *Physics Today* **54**, 37–42 (2001).
24. Blatt, R., Häffner, H., Roos, C., Becher, C. & Schmidt-Kaler, F. *Quantum entanglement and information processing, Les Houches Summer School 2003, Session LXXIX*, chap. Quantum information processing in ion traps I (Elsevier, 2004).
25. Wineland, D. J. *Quantum entanglement and information processing, Les Houches Summer School 2003, Session LXXIX*, chap. Quantum information processing in ion traps II (Elsevier, 2004).
26. Leibfried, D., Blatt, R., Monroe, C. & Wineland, D. Quantum dynamics of single trapped ions. *Rev. Mod. Phys.* **75**, 281 (2003).
27. Wineland, D. J. *et al.* Experimental issues in coherent quantum-state manipulation of trapped atomic ions. *J. Res. Natl. Inst. Stand. Technol.* **103**, 259–328 (1998).
28. Allen, L. C. & Eberly, J. H. *Optical Resonance and Two-Level Atoms* (Dover Publications Inc., 1987).

29. Diedrich, Bergquist, Itano & Wineland. Laser cooling to the zero-point energy of motion. *Phys. Rev. Lett.* **62**, 403–406 (1989).
30. Dehmelt, H. G. Mono-ion oscillator as potential ultimate laser frequency standard. *IEEE Trans. Instrum. Meas.* **IM-31**, 83–87 (1982).
31. Barenco *et al.* Elementary gates for quantum computation. *Phys. Rev. A* **52**, 3457–3467 (1995).
32. Monroe, Meekhof, King, Itano & Wineland. Demonstration of a fundamental quantum logic gate. *Phys. Rev. Lett.* **75**, 4714–4717 (1995).
33. Schmidt-Kaler, F. *et al.* Realization of the Cirac-Zoller controlled-NOT quantum gate. *Nature* **422**, 408–411 (2003). URL <http://dx.doi.org/10.1038/nature01494>.
34. Schmidt-Kaler, F. *et al.* How to realize a universal quantum gate with trapped ions. *Appl. Phys. B* **77**, 789 (2003).
35. Riebe, M. *et al.* Process tomography of ion trap quantum gates. *Phys. Rev. Lett.* **97**, 220407 (2006). URL <http://link.aps.org/abstract/PRL/v97/e220407>.
36. Turchette, Q. A. *et al.* Deterministic entanglement of two trapped ions. *Phys. Rev. Lett.* **81**, 3631–3634 (1998).
37. Rowe, M. A. *et al.* Experimental violation of a Bell's inequality with efficient detection. *Nature* **409**, 791–794 (2001). URL <http://dx.doi.org/10.1038/35057215>.

38. Roos, C. F. *et al.* Bell states of atoms with ultralong lifetimes and their tomographic state analysis. *Phys. Rev. Lett.* **92**, 220402 (2004).
39. Sackett *et al.* Experimental entanglement of four particles. *Nature* **404**, 256–259 (2000).
URL <http://dx.doi.org/10.1038/35005011>.
40. Clauser, J. F., Horne, M., Shimony, A. & Holt, R. A. Proposed experiment to test local hidden-variable theories. *Phys. Rev. Lett.* **23**, 880–884 (1969).
41. Clauser, J. F. & Shimony, A. Bell's theorem: experimental tests and implications. *Rep. Prog. Phys.* **41**, 1881–1926 (1978).
42. Moehring, D. L., Madsen, M. J., Blinov, B. B. & Monroe, C. Experimental Bell inequality violation with an atom and a photon. *Phys. Rev. Lett.* **93**, 090410 (2004).
43. Schrödinger, E. Die gegenwärtige Situation in der Quantenmechanik. *Naturwissenschaften* **23**, 807 (1935).
44. Greenberger, D. M., Horne, M. A. & Zeilinger, A. *Bell's Theorem, Quantum Theory and Conceptions of the Universe*, chap. Going beyond Bell's Theorem, 69–72 (Kluwer Academic, Dordrecht, 1989).
45. DiVincenzo & Shor. Fault-tolerant error correction with efficient quantum codes. *Phys. Rev. Lett.* **77**, 3260–3263 (1996).
46. Steane, A. Error correcting codes in quantum theory. *Phys. Rev. Lett.* **77**, 793–797 (1996).

47. Zhao, Z. *et al.* Experimental demonstration of five-photon entanglement and open-destination teleportation. *Nature* **430**, 54–58 (2004).
48. Hillery, M., Buzek, V. & Berthiaume, A. Quantum secret sharing. *Phys. Rev. A* **59**, 1829–1834 (1999).
49. Bollinger, Itano, Wineland & Heinzen. Optimal frequency measurements with maximally correlated states. *Phys. Rev. A* **54**, R4649–R4652 (1996).
50. Leibfried, D. *et al.* Toward Heisenberg-limited spectroscopy with multiparticle entangled states. *Science* **304**, 1476–1478 (2004). URL <http://dx.doi.org/10.1126/science.1097576>.
51. Leibfried, D. *et al.* Creation of a six-atom 'Schrödinger cat' state. *Nature* **438**, 639–642 (2005).
52. Roos, C. F. *et al.* Control and measurement of three-qubit entangled states. *Science* **304**, 1478–1480 (2004). URL <http://dx.doi.org/10.1126/science.1097522>.
53. Dür, W., Vidal, G. & Cirac, J. I. Three qubits can be entangled in two inequivalent ways. *Phys. Rev. A* **62**, 062314 (2000).
54. Cabello, A. Bell's theorem with and without inequalities for the three-qubit Greenberger-Horne-Zeilinger and W states. *Phys. Rev. A* **65**, 032108 (2002).
55. Häffner, H. *et al.* Scalable multiparticle entanglement of trapped ions. *Nature* **438**, 643–646 (2005).

56. Deutsch, D. & Jozsa, R. Rapid solution of problems by quantum computation. *Proc. R. Soc. Lond. A* **439**, 553–558 (1992).
57. Chuang, I. L., Vandersypen, L. M. K., Zhou, X., Leung, D. W. & Lloyd, S. Experimental realization of a quantum algorithm. *Nature* **393**, 143 (1998).
58. Gulde, S. *et al.* Implementation of the Deutsch-Jozsa algorithm on an ion-trap quantum computer. *Nature* **421**, 48–50 (2003). URL <http://dx.doi.org/10.1038/nature01336>.
59. Bennett *et al.* Teleporting an unknown quantum state via dual classical and Einstein-Podolsky-Rosen channels. *Phys. Rev. Lett.* **70**, 1895–1899 (1993).
60. Barrett, M. D. *et al.* Deterministic quantum teleportation of atomic qubits. *Nature* **429**, 737–739 (2004). URL <http://dx.doi.org/10.1038/nature02608>.
61. Riebe, M. *et al.* Deterministic quantum teleportation with atoms. *Nature* **429**, 734–737 (2004).
62. Gottesman, D. & Chuang, I. L. Demonstrating the viability of universal quantum computation using teleportation and single-qubit operations. *Nature* **402**, 390–393 (1999).
63. Reichle, R. *et al.* Experimental purification of two-atom entanglement. *Nature* **443**, 838–841 (2006). URL <http://dx.doi.org/10.1038/nature05146>.
64. Chiaverini, J. *et al.* Realization of quantum error correction. *Nature* **432**, 602–605 (2004). URL <http://dx.doi.org/10.1038/nature03074>.

65. Chiaverini, J. *et al.* Implementation of the semiclassical quantum Fourier transform in a scalable system. *Science* **308**, 997–1000 (2005). URL <http://dx.doi.org/10.1126/science.1110335>.
66. Riebe, M. *et al.* Deterministic entanglement swapping in an ion trap quantum computer. Submitted for publication, Innsbruck 2008.
67. Grover, L. K. Quantum mechanics helps in searching for a needle in a haystack. *Phys. Rev. Lett.* **79**, 325–328 (1997).
68. Wineland, D. J., Bollinger, J. J., Itano, W. M., Moore, F. L. & Heinzen, D. J. Spin squeezing and reduced quantum noise in spectroscopy. *Phys. Rev. A* **46**, R6797–R6800 (1992).
69. Itano, W. M. *et al.* Quantum projection noise: population fluctuations in two-level systems. *Phys. Rev. A* **47**, 3554–3570 (1993).
70. Meyer, V. *et al.* Experimental demonstration of entanglement-enhanced rotation angle estimation using trapped ions. *Phys. Rev. Lett.* **86**, 5870–5873 (2001).
71. Leibfried, D. *et al.* Trapped-ion quantum simulator: experimental application to nonlinear interferometers. *Phys. Rev. Lett.* **89**, 247901 (2002).
72. Huelga, S. F. *et al.* Improvement of frequency standards with quantum entanglement. *Phys. Rev. Lett.* **79**, 3865–3868 (1997).
73. André, A., Sørensen, A. & Lukin, M. D. Stability of atomic clocks based on entangled atoms. *Phys. Rev. Lett.* **92**, 230801–1–4 (2004).

74. Schaetz, T. *et al.* Enhanced quantum state detection efficiency through quantum information processing. *Phys. Rev. Lett.* **94**, 010501 (2005).
75. Hume, D. B., Rosenband, T. & Wineland, D. J. High-fidelity adaptive qubit detection through repetitive quantum nondemolition measurements. *Phys. Rev. Lett.* **99**, 120502–1 – 120502–4 (2007).
76. Rosenband, T. *et al.* Observation of the 1s_0 to 3p_0 clock transition in $^{27}\text{Al}^+$. *Phys. Rev. Lett.* **98**, 220801–1 – 220801–4 (2007).
77. Haroche, S. & Raimond, J.-M. *Exploring the Quantum - Atoms, Cavities, and Photons* (Oxford University Press, 2006).
78. Roos, C. F., Chwalla, M., Kim, K., Riebe, M. & Blatt, R. 'Designer atoms' for quantum metrology. *Nature* **443**, 316–319 (2006). URL <http://dx.doi.org/10.1038/nature05101>.
79. Benhelm, J., Kirchmair, G., Roos, C. F. & Blatt, R. Towards fault-tolerant quantum computing with trapped ions. *Nature Physics* (2008).
80. Ozeri, R. *et al.* Errors in trapped-ion quantum gates due to spontaneous photon scattering. *Physical Review A* **75**, 042329 (2007). URL <http://link.aps.org/abstract/PRA/v75/e042329>.
81. Zhu, S.-L., Monroe, C. & Duan, L. M. Arbitrary-speed quantum gates within large ion crystals through minimum control of laser beams. *quant-ph/0508037* (2006).

82. Duan, L.-M. Scaling ion trap quantum computation through fast quantum gates. *Phys. Rev. Lett.* **93**, 100502 (2004).
83. DeVoe, R. G. Elliptical ion traps and trap arrays for quantum computation. *Phys. Rev. A* **58**, 910–914 (1998).
84. Cirac & Zoller. A scalable quantum computer with ions in an array of microtraps. *Nature* **404**, 579–581 (2000). URL <http://dx.doi.org/10.1038/35007021>.
85. Kielpinski, D., Monroe, C. & Wineland, D. J. Architecture for a large-scale ion-trap quantum computer. *Nature* **417**, 709–711 (2002). URL <http://dx.doi.org/10.1038/nature00784>.
86. Cirac, I., Zoller, P., Kimble, J. & Mabuchi, H. Quantum state transfer and entanglement distribution among distant nodes in a quantum network. *Phys. Rev. Lett.* **78**, 3221 (1997).
87. Duan, L.-M. & Kimble, H. J. Scalable photonic quantum computation through cavity-assisted interactions. *Phys. Rev. Lett.* **92**, 127902 (2004).
88. Duan, L.-M. *et al.* Probabilistic quantum gates between remote atoms through interference of optical frequency qubits. *Phys. Rev. A* **73**, 062324 (2006).
89. Moehring, D. L. *et al.* Entanglement of single-atom quantum bits at a distance. *Nature* **449**, 68–71 (2007).
90. Rowe, M. *et al.* Transport of quantum states and separation of ions in a dual rf ion trap. *Quant. Inf. Comp.* **2**, 257–271 (2002).

91. Hucul, D. *et al.* On the transport of atomic ions in linear and multidimensional trap arrays. *arXiv:quant-ph/070217* (2007).
92. Huber, G. *et al.* Transport of ions in a segmented linear paul trap in printed-circuit-board technology. *arXiv:quant-ph/0711.2947* (2007).
93. Rohde, H. *et al.* Sympathetic ground-state cooling and coherent manipulation with two-ion crystals. *J. Opt. Soc. Am. B* **3**, S34–S41 (2001).
94. Blinov, B. B. *et al.* Sympathetic cooling of trapped Cd^+ isotopes. *Phys. Rev. A* **65**, 040304–1–4 (2002).
95. Barrett, M. D. *et al.* Sympathetic cooling of $^9\text{Be}^+$ and $^{24}\text{Mg}^+$ for quantum logic. *Phys. Rev. A* **68**, 042302–1–8 (2003).
96. Turchette, Q. A. *et al.* Heating of trapped ions from the quantum ground state. *Phys. Rev. A* **61**, 0634318 (2000).
97. Deslauriers, L. *et al.* Scaling and suppression of anomalous heating in ion traps. *Phys. Rev. Lett.* **97**, 103007 (2006).
98. Leibbrandt, D., Yurke, B. & Slusher, R. Modeling ion trap thermal noise decoherence. *Quantum Information & Communication* **7**, 52–72 (2007).
99. Deslauriers, L. *et al.* Zero-point cooling and low heating of trapped $^{111}\text{Cd}^+$ ions. *Phys. Rev. A* **70**, 043408–1–5 (2004).

100. Epstein, R. J. *et al.* Simplified motional heating rate measurements of trapped ions. *Phys. Rev. A* **76**, 033411–1–5 (2007).
101. Labaziewicz, J. *et al.* Suppression of heating rates in cryogenic surface-electrode ion traps. *Phys. Rev. Lett.* **100**, 013001–1–4 (2008).
102. Stick, D. *et al.* Ion trap in a semiconductor chip. *Nature Physics* **2**, 36–39 (2006).
103. Chiaverini, J. *et al.* Surface-electrode architecture for ion-trap quantum information processing. *Quantum Information and Computation* **5**, 419 (2005).
104. Seidelin, S. *et al.* Microfabricated surface-electrode ion trap for scalable quantum information processing. *Phys. Rev. Lett.* **96**, 253003 (2006).
105. Kim, J. *et al.* System design for large-scale ion trap quantum information processor. *Quantum Information & Communication* **5**, 515–537 (2005).
106. Leibfried, D., Knill, E., Ospelkaus, C. & Wineland, D. J. Transport quantum logic gates for trapped ions. *Phys. Rev. A* **76**, 032324–1–12 (2007).
107. Wunderlich, C. & Balzer, C. Quantum measurements and new concepts for experiments with trapped ions. *Adv. Atomic, Molecular, and Optical Physics* **49**, 293 (2003).
108. Porras, D. & Cirac, J. I. Quantum manipulation of trapped ions in two dimensional Coulomb crystals. *Phys. Rev. Lett.* **96**, 250501–1–4 (2006).
109. Taylor, J. M. & Calarco, T. Wigner crystals of ions as quantum hard drives. *arXiv:0706.1951* (2007).

110. Mølmer, K. & Sørensen, A. Multiparticle entanglement in a hot ion trap. *Phys. Rev. Lett.* **82**, 1835 (1999).
111. Milburn, G. J., Schneider, S. & James, D. F. Ion trap quantum computing with warm ions. *Fortschr. Physik* **48**, 801 (2000).
112. Solano, E., de Matos Filho, R. L. & Zagury, N. Mesoscopic superpositions of vibronic collective states of n trapped ions. *Phys. Rev. Lett.* **87**, 060402 (2001).
113. Leibfried, D. *et al.* Experimental demonstration of a robust, high-fidelity geometric two ion-qubit phase gate. *Nature* **422**, 412–415 (2003). URL <http://dx.doi.org/10.1038/nature01492>.
114. Haljan, P. C. *et al.* Entanglement of trapped-ion clock states. *Phys. Rev. A* **72**, 062316 (2005).
115. Home, J. P. *et al.* Deterministic entanglement and tomography of ion spin qubits **8**, 188 (2006).
116. Nielsen, M. A. & Chuang, I. L. *Quantum Computation and Quantum Information* (Cambridge Univ. Press, Cambridge, 2000).
117. Hensinger, W. K. *et al.* T-junction ion trap array for two-dimensional ion shuttling storage, and manipulation. *Appl. Phys. Lett.* **88**, 034101 (2006).

Addendum

Competing Interests The authors declare that they have no competing financial interests.

Correspondence Correspondence and requests for materials should be addressed to RB.

(email:Rainer.Blatt@uibk.ac.at).

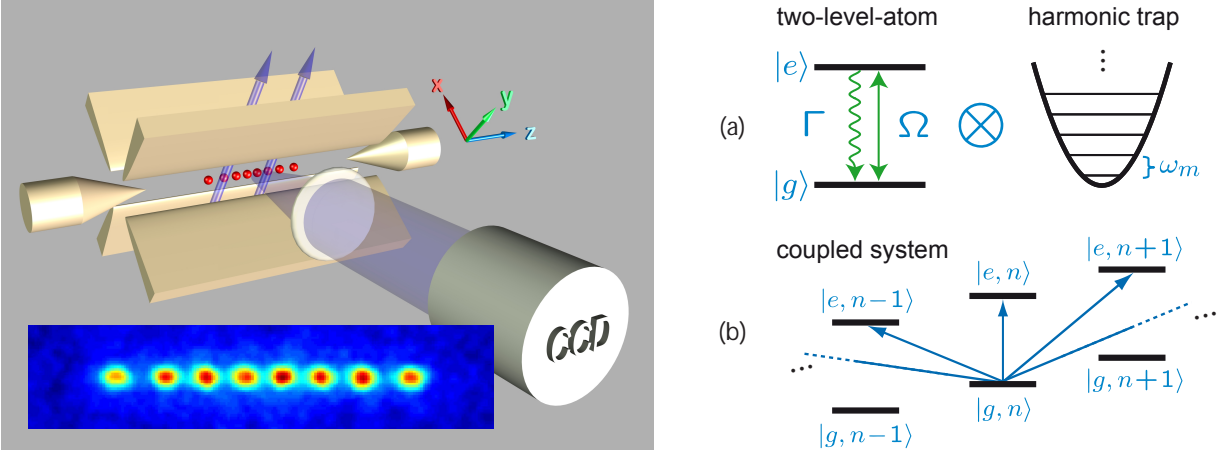


Figure 1: Left: Linear ion trap with individually addressed $^{40}\text{Ca}^+$ ions. In the inset photograph, the spacing of the two center ions is $\sim 8 \mu\text{m}$. Such an electrode arrangement provides a three-dimensional nearly harmonic well characterized for a single ion by three frequencies²⁶ ω_x, ω_y and ω_z , where x, y, z denote the confining potential axes, with z pointing along the trap axis and x, y in the transverse directions. Due to the Coulomb coupling between multiple ions, the motion is best described in terms of normal modes; a string of ions can therefore be viewed as a pseudo-molecule. Generally, the normal-mode frequencies are different, and we can access a particular mode by spectral selection. Right: (a) Two-level atom coupled to a harmonic trap. (b) Joint level system exhibiting multiple resonance frequencies.

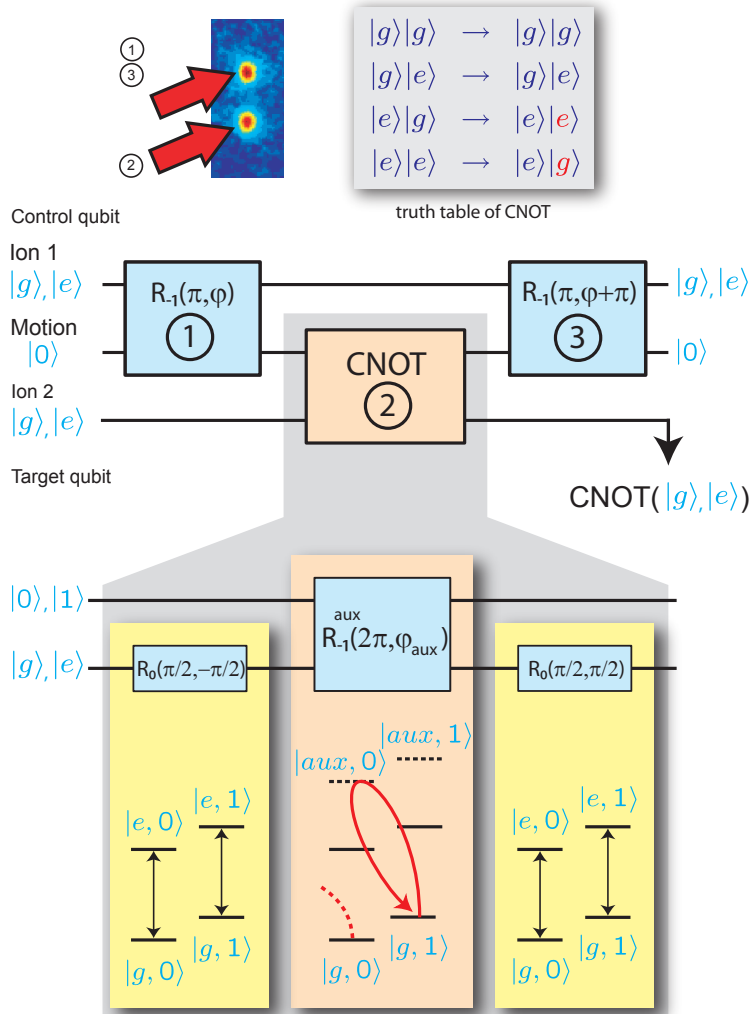


Figure 2: CNOT-gate operation with two trapped ions: Consider two ions in the same trap initially prepared in their motional ground state. In step (1) a red-sideband pulse $R_{-1}(\theta, \varphi)$ applied to the first ion (control qubit) maps the excited state amplitude of this ion to the first excited state of a selected motional mode as indicated in the upper part (SWAP operation). In step (2) a CNOT-gate operation is implemented between the motion qubit and the spin state of (target qubit) ion 2. Finally, in step (3) the first step is reversed, thereby restoring the initial spin state of ion 1 and returning the motion to its ground state. The lower part shows the actual pulse sequence of the CNOT-operation, for details see text.

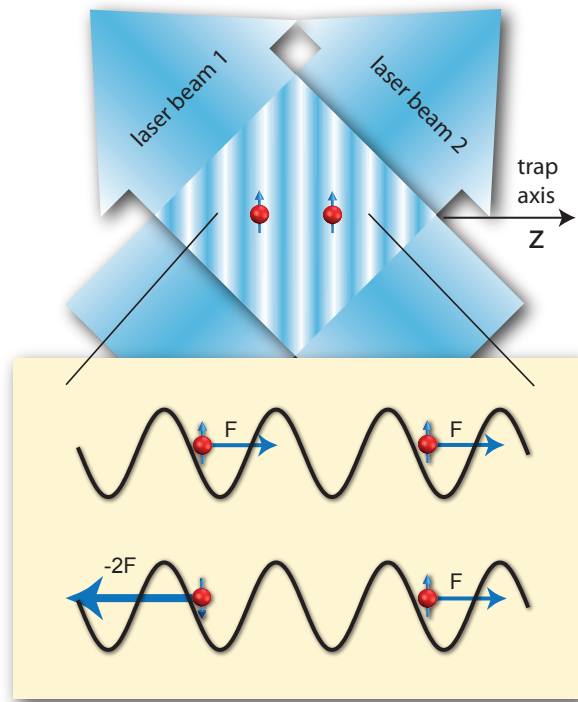


Figure 3: Two-qubit phase gate. The gate relies on the fact that when a selected mode of the ions' motion is displaced in phase space about a closed path, the ions' wave function picks up a phase proportional to the enclosed area. If this displacement depends on the ions' qubit states, entanglement is generated.¹¹⁰⁻¹¹³ We can implement this state-dependent displacement with optical dipole forces resulting from laser-beam intensity gradients, as depicted above. In this example, an intensity standing wave is created with two laser beams, and the horizontal spacing of the ions is made to be an integral number of wavelengths of the intensity pattern. The pattern sweeps across the ions at the difference frequency of the beams, chosen to be near the stretch-mode frequency. If $|g\rangle$ and $|e\rangle$ feel different dipole forces, then only the $|g\rangle|e\rangle$ and $|e\rangle|g\rangle$ components of the ions' wave function are displaced in (stretch-mode) phase space. By making the trajectories closed and choosing the size of the displacements appropriately, the wave function is unchanged except for an $e^{i\pi/2}$ phase shift on the $|g\rangle|e\rangle$ and $|e\rangle|g\rangle$ states, the desired phase gate. Such gate operations have been implemented with trapped ${}^9\text{Be}^+$ ions¹¹³, and in a similar way with ${}^{111}\text{Cd}^+$ ions¹¹⁴ and ${}^{40}\text{Ca}^+$ ions.^{79,115}

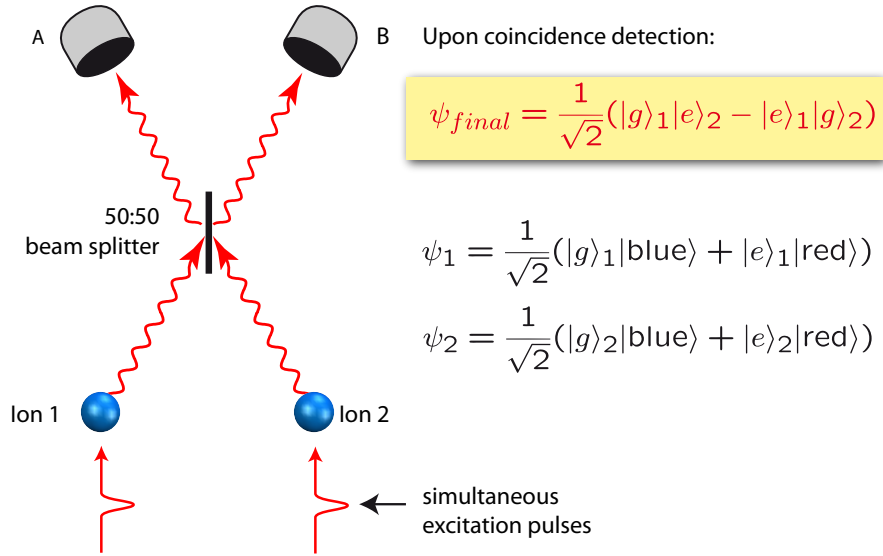


Figure 4: Projective Entanglement: In this example (following Ref. ⁸⁹), we assume that the qubits of two ions (blue spheres) are encoded in hyperfine levels of their electronic ground states. These qubits are first prepared in superposition states $\frac{1}{\sqrt{2}}(|g\rangle + |e\rangle)$. When excited with laser pulses short enough that both qubit levels undergo (single-photon) scattering, the frequencies (denoted red and blue) of the emitted photons along a particular direction are correlated with the qubit states, as indicated for entangled states ψ_1 and ψ_2 . If these photons are made to interfere on a beam splitter and detected, in the instances where photons are simultaneously detected at A and B, the ions are projected into the Bell state ψ_{final} even though the atoms have not directly interacted. For many such experiments, photons do not reach the detectors; however, when photons are coincidentally detected, this “heralds” the formation of the entangled state ψ_{final} , which can then be saved and used later. One potential use is for entanglement-assisted communication between the locations 1 and 2.

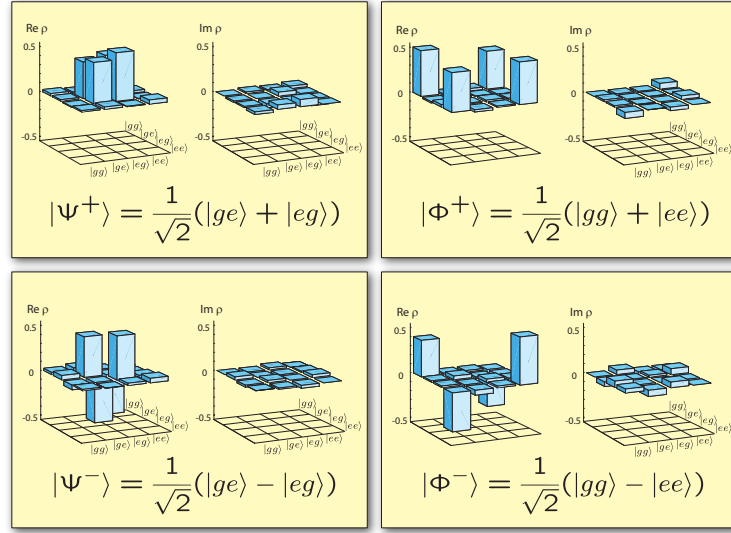


Figure 5: Real and imaginary parts of the density matrices obtained for Bell states prepared deterministically with two trapped Ca^+ ions. The states were analyzed by use of quantum state tomography which is a measurement technique that gives access to all the information that is necessary to describe any quantum state by means of its density matrix. From the results, the density matrix of the state in question can be reconstructed¹¹⁶. To see the idea, note that the density matrix for a single qubit can be represented by $\rho = \frac{1}{2}(I + \sum_i \langle \sigma_i \rangle \sigma_i)$ (with Pauli matrices $\sigma_i, i = x, y, z$ and the identity I). Measurements project a qubit onto its energy eigenstates, which is equivalent to measuring $\langle \sigma_z \rangle$. In order to determine $\langle \sigma_{x,y} \rangle$, an additional rotation of the Bloch sphere is applied prior to the measurement. The tomography procedure can be extended to N qubits, which requires measuring on the order of 4^N expectation values. Experimentally, due to statistical errors, the measured expectation values can result in an unphysical density matrix exhibiting negative eigenvalues. This is avoided by fitting the measured expectation values by use of a maximum likelihood method and finding the most likely density matrix describing the state³⁸.

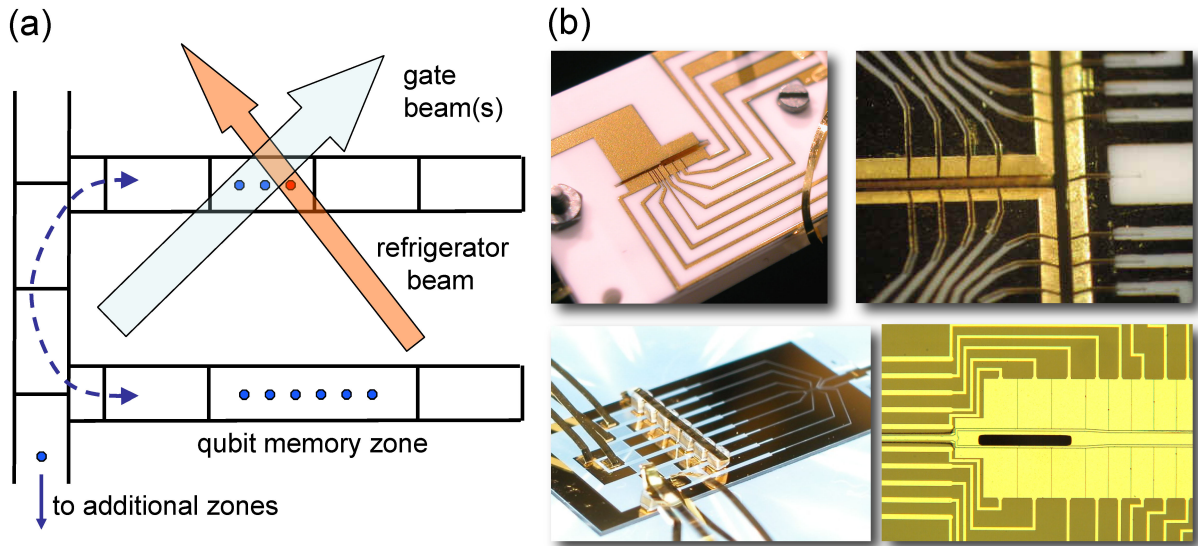


Figure 6: Multi zone trap arrays. (a) The trap zones are shown schematically as rectangles. Ions can be separated and moved to specific zones with control potentials applied between the segments. Because ions will heat from transport and noisy ambient electric fields, refrigerator ions are used to cool the ions prior to gate operations. (b) Examples of trap electrode configurations. Upper left: two-layer, linear six-zone trap in which entangled ions could be separated and used for algorithm demonstrations including teleportation⁶⁰ (width of narrow slot = $200 \mu\text{m}$). Upper right: three-layer, 2-D multi-zone trap which can be used to switch ion positions¹¹⁷(slot width = $200 \mu\text{m}$). Lower left: single zone trap where all electrodes lie in a plane; this can considerably simplify fabrication¹⁰⁴. Lower right: linear, multi-zone, planar trap fabricated on silicon (width of open slot for loading ions $\simeq 95\mu\text{m}$), which can enable electronics to be fabricated on board [R. Slusher, private communication].